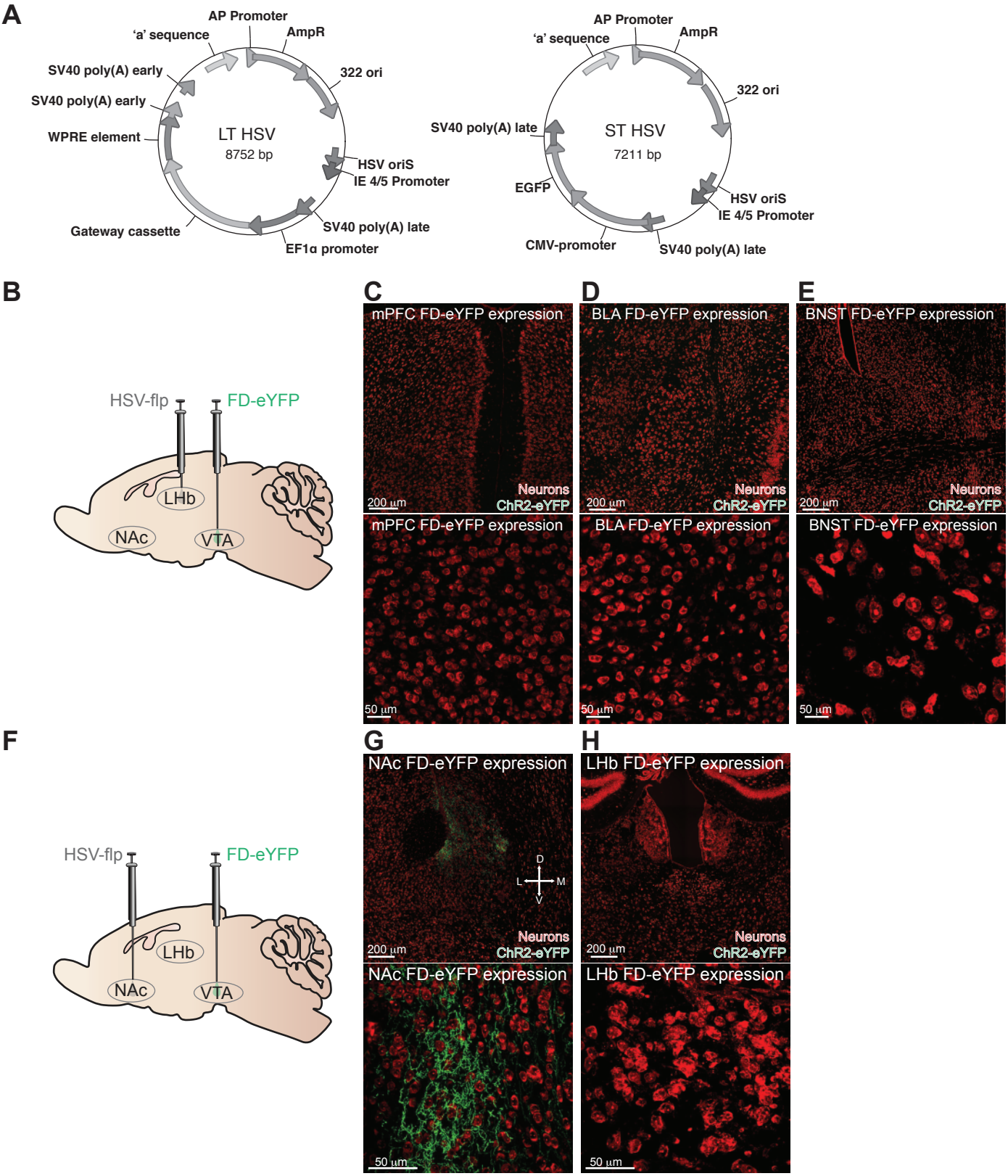

Figure S1, related to Figure 1. LHb-projecting VTA dopaminergic neurons do not send collaterals to other dopaminergic target regions (A) HSV vector maps. LT HSV virus encoding a cre inducible flp recombinase was modified from previously published ST HSV vectors. LT HSV results in longer term expression of introduced transgenes into neurons compared to standard (ST) HSV vectors. (B) Schematic of HSV-EF1α-LS1L-flp (HSV-flp) and AAV5-EF1α-fdhChR2(H134R)-eYFP (FD-eYFP) viral injections. (C-E) Coronal confocal image showing eYFP+ expression in the mPFC (C), BLA (D), and BNST (E) following injection of HSV-flp into the LHb and FD-eYFP into the VTA of *TH*:IRES:Cre mice. (F) Schematic of HSV-flp and FD-eYFP viral injections. (G,H) Coronal confocal image showing eYFP+ expression in the NAc (G) and LHb (H) following injection of HSV-flp into the LHb and FD-eYFP into the VTA of *TH*:IRES:Cre mice.

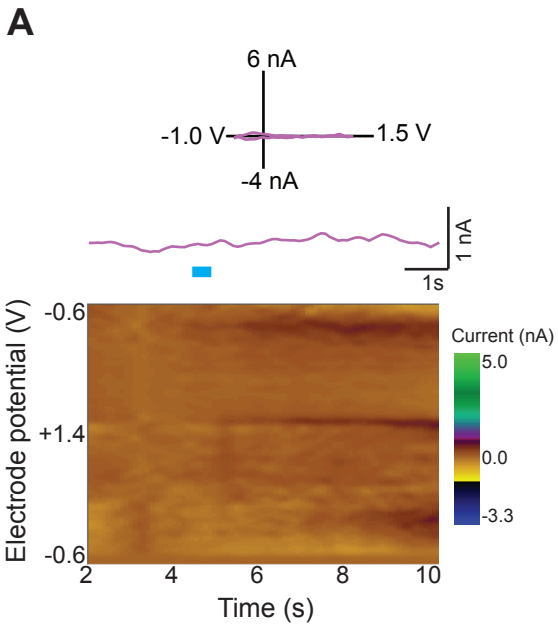

Figure S2, related to Figure 4. *TH*$^{VTA-LHb}$ neurons do not release detectable dopamine in the LHb
(A) Fast-scan cyclic voltammetric recordings of optically-evoked dopamine release in *TH*$^{VTA-LHb}$::ChR2 brain slices with sensitivity for dopamine increased. Slices were incubated in 1 μM GBR12909 and 10 μM raclopride for at least 1 hr before recording. 10 min prior to recording, slices were pre-perfused with 10 μM L-Dopa. The potential applied to the electrode was ramped from -0.6 V to +1.4 V to -0.6 V versus an Ag/AgCl reference wire at a rate of 400 V/s. Top: Example trace of voltammetric recording from LHb brain slice. Inset: Background-subtracted cyclic voltammograms showing an electrochemical signal that is not indicative of oxidized dopamine. Bottom: Consecutive background-subtracted voltammograms recorded over the 8-s interval. Applied potential (E_{apps} versus Ag/AgCl reference electrode) is shown on Y-axis. Time at which each voltammogram was recorded is shown on X-axis. Current changes are color coded.

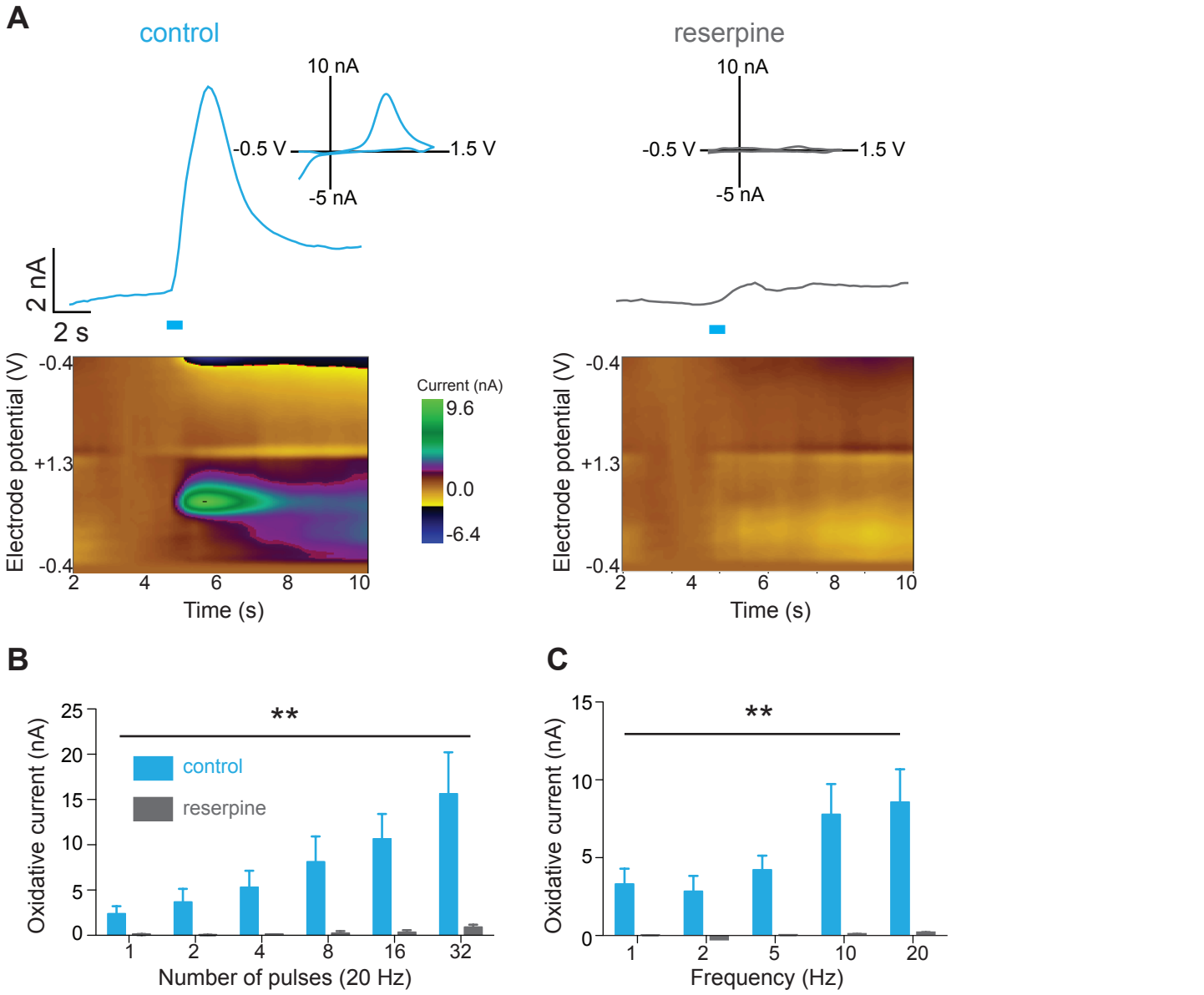

Figure S3, related to Figure 5. Reserpine prevents electrically-evoked dopamine release (A) Fast-scan cyclic voltammetric recordings of electrically-evoked dopamine release in control wild-type mice (left) and wild-type mice injected with 5 mg/kg reserpine (right). Top: Example traces of voltammetric recordings from NAc brain slices. Inset: Background-subtracted cyclic voltammograms showing an electrochemical signal indicative of oxidized dopamine. Bottom: Consecutive background-subtracted voltammograms recorded over the 8-s interval for control mice (left) and reserpine-treated mice (right). Applied potential (E_{apps} versus Ag/AgCl reference electrode) is shown on Y-axis. Time at which each voltammogram was recorded is shown on X-axis. Current changes are color coded. (B) Light-evoked current is significantly higher in the control slices than reserpine-treated slices for all measured number of light pulses ($F[5,1] = 11.06$, $p < 0.001$). (C) Light-evoked current is significantly higher in control mice than reserpine-treated slices for all measured frequencies ($F[4,1] = 47.09$, $p < 0.001$). Error bars represent s.e.m. **$p < 0.01$ (ANOVA followed by Bonferroni post-hoc comparisons).

A

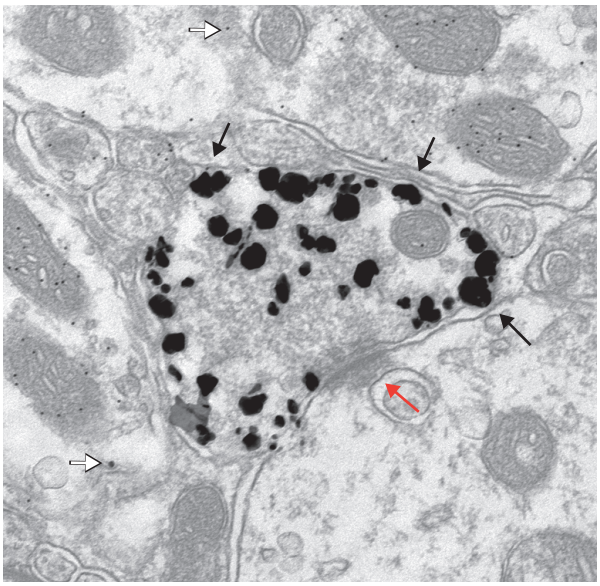

Figure S4, related to Figure 5. GABA-negative asymmetric *TH*$^{VTA\text{-}LHb}$::ChR2 synapse. (A) Electron micrograph showing *TH*$^{VTA\text{-}LHb}$::ChR2 presynaptic terminal, as defined by large silver-enhanced particles (black arrows) making an asymmetric synapse (red arrow pointing to postsynaptic density). GABA (white arrows) is located in neighboring synapses, but not in *TH*$^{VTA\text{-}LHb}$::ChR2 presynaptic terminal.

Stamatakis et al., Supplemental Figure 5

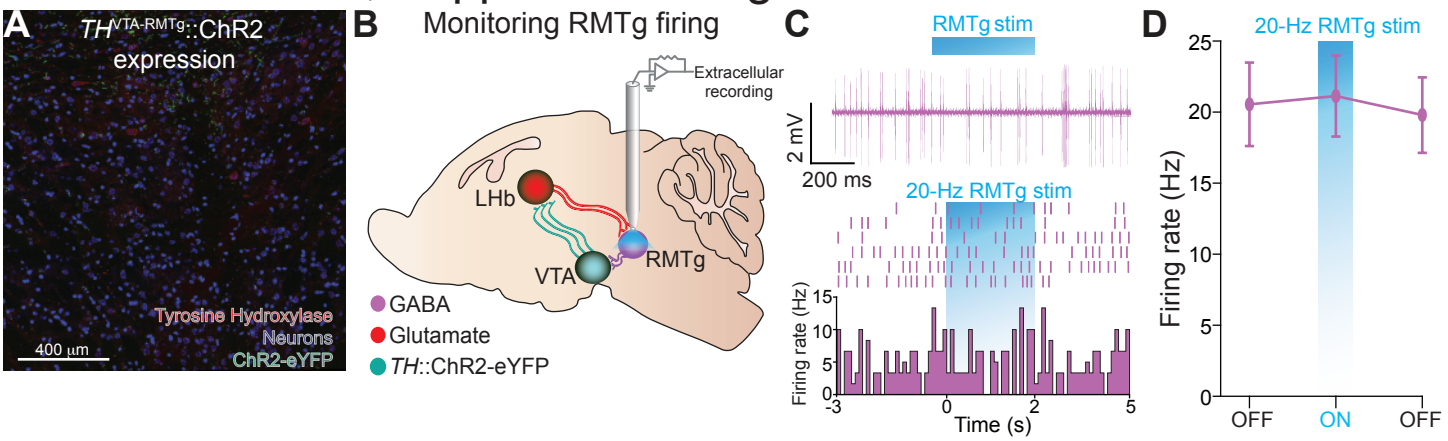

Figure S5, related to Figure 6. Confocal image of coronal section showing expression of ChR2-eYFP in the RMTg following injection of Cre-inducible virus into the VTA of a TH-IRES-Cre (*TH*^{VTA}::ChR2) mouse. We found that 3.02 ± 0.422 % of neurons were TH+. We observed very minimal ChR2-eYFP expression in RMTg brain slices (less than 3 neurons per slice). n = 4 slices from n = 4 mice. (B) Schematic detailing RMTg *in vivo* recordings paired with optical stimulation of the recording region. (C) Representative trace from a single non-optically excitable RMTg unit (top) and its representative peri-event histogram and raster (bottom) showing no responses to optical stimulation of the RMTg. (D) The average firing rate of RMTg neurons did not significantly alter during 20-Hz optical stimulation when compared to the time epochs without stimulation ($F[2,15] = 0.05675$, $p = 0.9450$, n = 3 mice, n = 6 units).

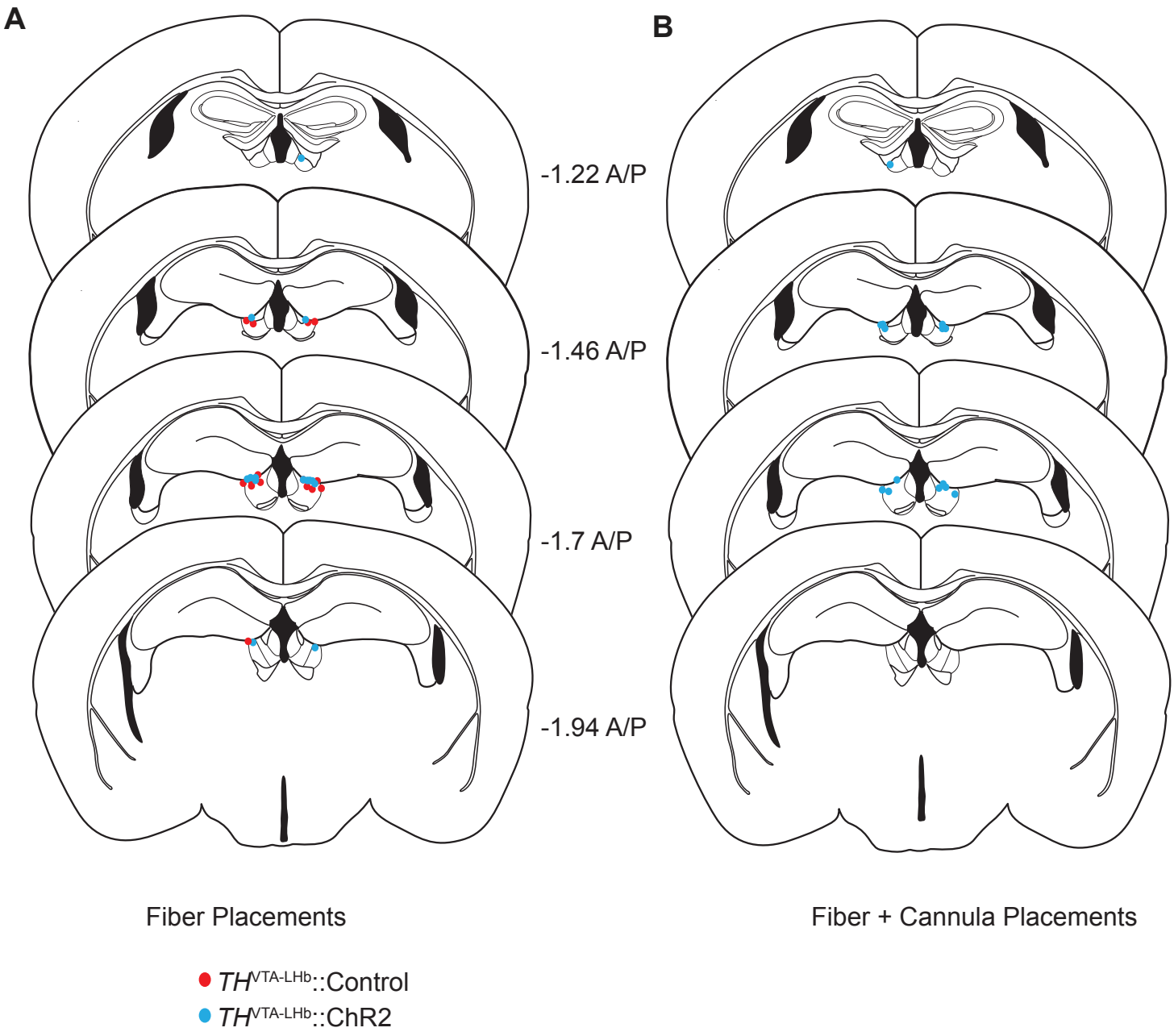

Figure S6, related to Figure 7. Optical fiber (A) and fiber+cannula (B) placements.

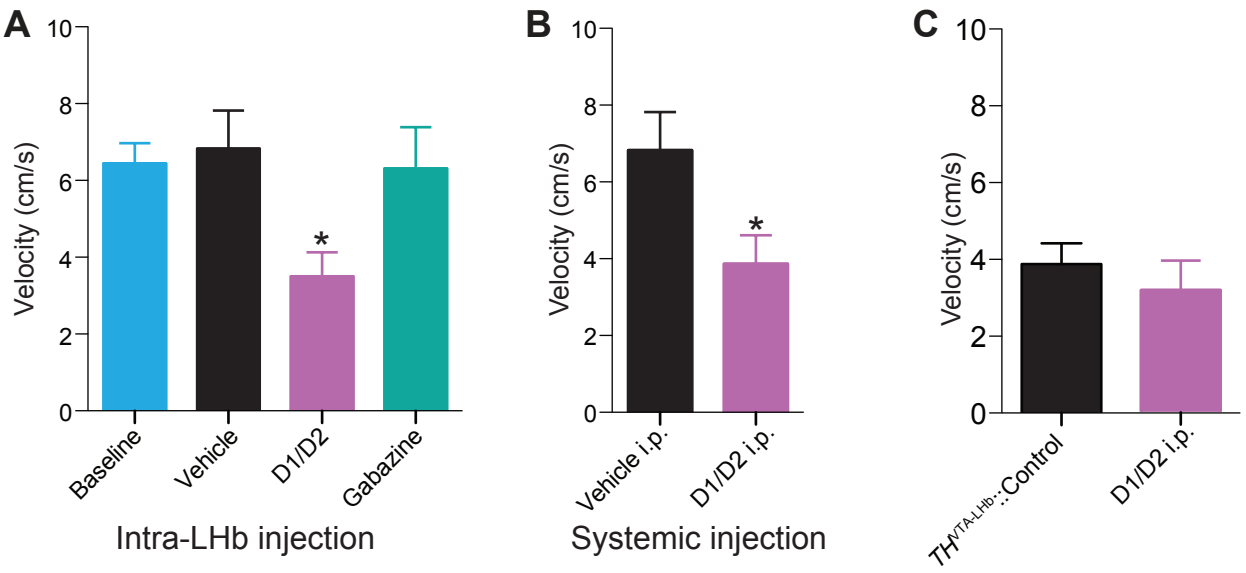

Figure S7, related to Figure 7. Velocity during real time place preference. (A) There was no significant difference in velocity following intra-LHb $GABA_A$ antagonist (gabazine) compared to vehicle ($t[16] = 0.4$, $p = 0.72$). Velocity was significantly decreased following intra-LHb dopamine antagonist (D1/D2) compared to vehicle ($t[16] = 2.8$, $p = 0.01$). (B) Velocity was significantly decreased following systemic dopamine antagonist (D1/D2) compared to vehicle ($t[14] = 2.3$, $p = 0.04$). (C) Velocity was not significantly different following systemic dopamine antagonist (D1/D2) compared to *TH*$^{VTA\text{-}LHb}$::Control mice ($t[13] = 0.77$, $p = 0.45$). All velocity measurements were taken across entire 20 minute session. Error bars represent s.e.m. *$p < 0.01$. n = 9 *TH*$^{VTA\text{-}LHb}$::ChR2 intra-LHb mice, n = 7 *TH*$^{VTA\text{-}LHb}$::ChR2 systemic injection mice, n = 8 *TH*$^{VTA\text{-}LHb}$::Control mice.

SUPPLEMENTAL EXPERIMENTAL PROCEDURES

Stereotactic coordinates. VTA coordinates (in mm from bregma): −3.1 anterior/posterior, ±0.4 medial/lateral, −5.0 dorsal/ventral. NAc coordinates (quadruple injections) at four different sites (in mm from bregma): +1.0 and 1.5 anterior/posterior, ±1.0 medial/lateral, −4.4 dorsal/ventral. LHb coordinates (quadruple injections) at four different sites (in mm from bregma): -1.3 and -1.9 anterior/posterior, ±0.44 medial/lateral, -3.44 dorsal/ventral. LHb fiber coordinates (in mm from bregma at 15º): -1.7 anterior/posterior, ±1.25 medial/lateral, -3.24 dorsal/ventral.

HSV vector construction. To optimize the transcriptional cassette in the ST HSV vector backbone, thereby creating LT HSV, the entire CMV-transgene-SV40 polyadenylation (pA) signal cassette in ST HSV was replaced with an optimized cassette that had been previously assembled. The ST HSV and LT HSV have different promoters. The hCMV-IE1 promoter in the ST HSV was derived from pEGFP-C1 (Clontech), whereas it has been replaced with the EF1α promoter in LT HSV. The LT HSV vector also contains base pairs 1064-1750 of the Woodchuck Hepatitis Virus post-transcriptional response element (WPRE; (Donello et al., 1998)) which contributes to stabilization of expression. The promoter is flanked on the 5' side by the HSV oriS and IE4/5 promoter, which are followed by a SV40 A signal. The 3' pA signal in ST HSV is the SV40 late pA signal, and was derived from pCI (Promega), whereas the 3' pA signal in LT HSV is the SV40 early pA signal.

Histology, immunohistochemistry, and confocal microscopy. Mice were anesthetized with pentobarbital, and transcardially perfused with PBS followed by 4% (w/v) paraformaldehyde in PBS. Brains were then removed and submerged in 4% paraformaldehyde for 24 hr and transferred to 30% sucrose in ddH2O for 48 hr. 40 μm brain sections were obtained and subjected to immunohistochemical staining for neuronal cell bodies (NeuroTrace Invitrogen; 640-nm excitation/660-nm emission or 435-nm excitation/455-nm emission), and/or tyrosine hydroxylase (Pel Freeze; made in sheep, 1:500). Brain sections were mounted, and z-stack and tiled images were captured on a Zeiss LSM 710 confocal microscope using a 20x, 40x, or 63x objective and analyzed using ZEN 2009 and ImageJ software. To quantify fluorescence intensity, images were acquired using identical pinhole, gain, and laser settings for all brain regions. Intensity was the quantified using a scale from 0-255 in Image J to determine mean intensity. For co-localization analysis, Coloc2 software (Fiji) was used. To determine optical fiber placement, tissue was imaged at 10X and 20X on an upright conventional fluorescent microscope.

Electron Microscopy. *TH*$^{VTA\text{-}LHb}$::ChR2 mice were deeply anesthetized and intracardially perfused with PBS followed by a mixture of 4% paraformaldehyde and 1% glutaraldehyde in 0.1 M phosphate buffer, pH 7.2 (PB). Brains were removed and postfixed overnight in the same fixative. 50 μm-thick coronal sections throughout the LHb were cut on a Vibratome and collected in PB. Epifluorescence screening of wet sections was performed to confirm appropriate fluorescent label of fibers in LHb. Sections were incubated at room temperature

on a shaker in 1% hydrogen peroxide for 10 min (to block endogenous peroxidases), 30 min in 10% normal donkey serum (to block nonspecific antibody binding), and then overnight in chicken anti-GFP IgG (1:5,000). The next day sections were rinsed, blocked in 2% normal donkey serum, and treated with biotinylated secondary antibody against chicken IgG (Jackson ImmunoResearch, 1:200). After one hour incubation, sections were rinsed and incubated in ExtrAvidin (Sigma, 1:5,000) followed by standard diaminobenzidine histochemistry (for pre-embedding immunoperoxidase), or Nanogold-conjugated streptavidin (Nanoprobes, 1:100) followed by silver enhancement with IntenSE M (Amersham) for visualization of pre-embedding immunogold. Immunoprocessed sections were incubated 1 h in osmium tetroxide solution (0.1-0.5% in PB), rinsed in maleate buffer (0.1 M, pH 6.0), then 1 h in uranyl acetate (1% in maleate). Sections were dehydrated through graded ethanol, infiltrated in Spurr's resin, and sandwiched between two sheets of ACLAR plastic. They were then flat embedded between glass slides and heat-polymerized at 60° C for 48 hours. After polymerization, bits of tissue were cut from LHb and glued to plastic blocks. Thin sections (~70 nm) were cut with a diamond knife and collected on 300 mesh nickel grids (Ted Pella) for further processing. For single-label analysis, sections were post-stained with uranyl acetate and Sato's lead; for double-label study, sections first processed for postembedding immunogold labeling for GABA, as previously described (Phend et al., 1992), before post-staining. Grids were examined in a Tecnai F12 transmission EM (FEI); images were collected with a Gatan 12-bit cooled CCD. Images were cropped and contrast adjusted using

Adobe Photoshop.

Patch-clamp Electrophysiology. Modified artificial cerebral spinal fluid contained (in mM): 225 sucrose, 119 NaCl, 1.0 NaH_2PO_4, 4.9 $MgCl_2$, 0.1 $CaCl_2$, 26.2 $NaHCo_3$, 1.25 glucose. Bicarbonate-buffered solution contained (in mM): 119 NaCl, 2.5 KCl, 1.0 NaH_2PO_4, 1.3 $MgCl_2$, 2.5 $CaCl_2$, 26.2 $NaHCO_3$, and 11 glucose (at 32-34°C). Potassium chloride internal solution contained (in mM): 135 KCl, 0.5 EGTA, 10 HEPES, 1.5 $MgCl_2$, in RNAse- and DNAse-free water (Millipore). Methanesulfonic acid contained (in mM): 117 Cs methanesulfonic acid, 20 HEPES, 0.4 EGTA, 2.8 NaCl, 5 TEA, 2 ATP, 0.2 GTP. Cesium chloride internal solution contained (in mM): 130 CsCl, 1 EGTA, 10 HEPES, 2 ATP, 0.2 GTP. Potassium gluconate internal solution contained (in mM): 130 K-gluconate, 10KCl, 10 HEPES, 10 EGTA, 2 $MgCl_2$, 2ATP, 0.2 GTP. pH = 7.35, 270-285 mOsm for all internal solutions. For voltage-clamp recordings, patch electrodes (3-5 MΩ) were back-filled with either a cesium methanesulfonic acid or cesium chloride internal solution. Cells were visualized using infrared differential contrast and fluorescence microscopy. For current-clamp and cell-attached recordings, patch electrodes (3-5 MΩ for current-clamp, 2-4 MΩ for cell-attached) were back-filled with a potassium gluconate internal solution. Whole-cell voltage-clamp, current-clamp, and cell-attached recordings of LHb or VTA dopaminergic neurons were made using an Axopatch 700B amplifier (Molecular Devices). For all optical stimulations, blue light (1 mW, 473 nm) was delivered through a 40X objective via a LED. Series resistance (15-25 MΩ) and/or input resistance were monitored online with a 5-mV hyperpolarizing step delivered between stimulation

sweeps. All data were filtered at 2kHz, digitized at 5-10kHz, and collected using pClamp10 software (Molecular Devices). For the autoreceptor experiment, following 5-10 min of baseline recording, 3 μm of the D2 agonist quinpirole was bath-applied for 5 min. For IPSCs, following 5-10 min of baseline recording, 1 mM of the K^+ channel blocker 4AP, and 1 μM of the Na^+ channel blocker TTX was bath-applied for 10 min, followed by a 10 min bath application of 10 μM of the $GABA_A$ receptor antagonist, SR-95531 (gabazine). IPSC and EPSC amplitudes were calculated by measuring the peak current from the average response from 6 sweeps during baseline and during each drug application. Cells that showed a > 20% change in the holding current or access resistance were excluded from analysis. To inhibit vesicular monoamine transporters *TH*^{VTA}::ChR2 mice were injected intraperitoneally with the irreversible *Vmat2* inhibitor reserpine (5 mg/kg) 24 h prior to slicing (Tritsch et al., 2012). Brain slices from these mice were prepared as described above, but were incubated in aCSF containing 1 μM reserpine. For the cell-attached recordings, following 5-10 min baseline recording, 10 μM of the D1 antagonist SCH23390 and 10 μM of the D2 antagonist raclopride were washed on for 10 min, followed by a 10 min bath application of 10 μM of the $GABA_A$ receptor antagonist, SR-95531 (gabazine).

Single-cell gene expression profiling. Extracted intracellular samples were profiled using the Single Cell-to-C_t Kit (Life Technologies). Briefly, intracellular contents were prepared individually in lysis solution containing DNase. The volume of lysis and DNase solution was reduced from the normal protocol to

compensate for the added volume of internal solution from each sample (approximately 3-5 μL). Reverse transcription of RNA to complementary DNA (cDNA) was then performed, followed by a multiplexed preamplification of all target genes using TaqMan Gene Expression Assays (Life Technologies). The assays used to detect the target genes in the VTA were the recommended exon-spanning assays for *Slc17a6* (vesicular glutamate transporter-2, *Vglut2*), *Slc32a1* (vesicular GABA transporter, *Vgat*), *GAD1/GAD2* (glutamate decarboxylase 1 and 2), *Slc18a2* (vesicular monoamine transporter-2, *Vmat2*), *DRD2,* (dopamine receptor D2), *DAT1* (dopamine transporter), *TH* (tyrosine hydroxylase), and *Rn18s* (Control). The house-keeping gene, *Rn18s*, is highly abundant in all cells, and was thus not preamplified in order to avoid a reduction of amplification of other cDNAs in the multiplexed sample. Next, qPCR was performed to obtain the C_t values of each target gene by using a StepOnePlus qPCR instrument (Life Technologies) using recommended amplification parameters for TaqMan based probes. Technical replicates from each individual biological sample were performed as well as those from tissue-stick control on the same 96-well plate. Thus, each 96 well plate contained 5 consecutively recorded cells and their 1 subsequent tissue-stick control sample.

Single-cell gene analysis. qPCR data obtained from a given cell were not included for analysis if their qPCR amplification curves were not consistent across technical replicates or if they did not display a predicted sigmoidal amplification curve. Additionally, tissue-stick controls did not display any expression of the profiled target genes following qPCR. Gene expression for

each neuron was normalized to the sample's Rn18s expression in order to account for the volume of each collected sample ($\Delta C_t = C_t^{gene} - C_t^{Rn18s}$). Gene expression for each neuron was then normalized and calculated as the difference between normalized gene expression of each gene and normalized average expression of that gene in $TH^{VTA\text{-}NAc}$ neurons ($\Delta\Delta C_t = \Delta C_t$ – Avg. $\Delta C_{t,VTA\text{-}NAc}$). These fold expression values for each gene were log transformed (Normalized gene amount relative to $TH^{VTA\text{-}NAc} = 2^{-\Delta\Delta Ct}$; (Livak and Schmittgen, 2001)) and analyzed with a non-parametric t test (Mann-Whitney). Only data from TH-GFP neurons that expressed TH were included in the analysis.

Fast-scan cyclic voltammetry. Electrochemical data were acquired using a custom-written software in LabVIEW and filtered at 1 kHz offline. 5-ms, 473-nm, 1-mW light pulses were delivered through a 40X objective via a high-powered LED (Thorlabs) to evoke dopamine release. 5 light pulses were delivered at 1, 2, 5, 10, and 20 Hz. At 20 Hz, 1, 2, 4, 8, 16, and 32 light pulses were delivered. Immediately after optical stimulation of the slice, background-subtracted cyclic voltammograms were generated, which were characteristic of dopamine (peak oxidation potential of 600-700 mV).

***In vivo* circuit activity mapping of the $TH^{VTA\text{-}LHb}$ pathway.** TH^{VTA}::ChR2 mice were anesthetized with choral hydrate (4% w/v. 480 mg/kg i.p.) and supplemental doses were provided as needed (4% w/v, 120 mg/kg i.p.) (Sigma). A homeothermic heating blanket (Harvard Apparatus, Holliston, MA) was used to maintain body temperature at ~ 37°C and lidocaine (2%) was applied to the

incision site (Akorn). A reference electrode was fixed within brain tissue and extracellular neural activity was recorded using glass recording electrodes (5-10 MΩ: and filled with 0.5 M NaCl). All recordings were amplified (Multiclamp 700B, Molecular Devices), bandpass filtered between 300 Hz and 16 kHz and sampled up to 40 kHz. Data acquisition and analysis was performed using pCLAMP software (Molecular Devices) and placements of recording electrode tips within the RMTg and VTA were verified with histological examination of brain tissue following the experiments.

Real-time place preference. *TH*$^{VTA\text{-}LHb}$::ChR2 and *TH*$^{VTA\text{-}LHb}$::Control mice bilaterally implanted with optical fibers aimed at the LHb were placed in a custom-made behavioral arena (50 × 50 × 25 cm black plexiglass) for 20 min. One counterbalanced side of the chamber was assigned as the stimulation side. At the start of the session, the mouse was placed in the non-stimulated side of the chamber. Every time the mouse crossed to the stimulation side of the chamber, 20-Hz constant laser stimulation was delivered until the mouse crossed back into the non-stimulation side. Percent time spent on the stimulation-paired and velocity was recorded via a CCD camera interfaced with Ethovision software (Noldus Information Technologies).

Intra-LHb injection of antagonists and photostimulation during the RTPP test. *TH*$^{VTA\text{-}LHb}$::ChR2 mice bilaterally implanted with a 26-gauge cannula coupled to an optical fiber aimed above the LHb were placed in the place-preference chamber and were run in the RTPP task to achieve a baseline

measurement. 24 hr following the baseline measurement, mice received intra-LHb bilateral 0.3 μL microinjections of vehicle (saline), a dopamine receptor antagonist cocktail (600 ng of SCH23390 to block D1 receptors and 100 ng raclopride to block D2 receptors in saline), or gabazine (5 ng in saline) counterbalanced across days. The injector needles (33-gauge steel tube, McMasters-Carr) extended approximately 1 mm past the cannula to ensure drug delivery 0.5 mm below the optical fiber. All drugs were infused at a rate of 1.5 μL/min. The injector remained in place for 2 min after infusion to ensure diffusion of drug into the LHb. Immediately after the infusion procedure, mice were placed into the RTPP chamber. Mice had at least 24 hours without manipulation between each LHb microinjection.

Systemic injection of antagonists and photostimulation during the RTPP test. 7 days following the intra-LHb microinjections, *TH*$^{VTA-LHb}$::ChR2 mice were given i.p. injections of either vehicle (saline) or a dopamine receptor antagonist cocktail (0.04 mg/kg SCH23390 and 0.075 mg/kg raclopride). 20 min following the injection, mice were placed into the RTPP chamber. Mice had at least 24 hr without manipulation between each injection.

Optical self-stimulation. *TH*$^{VTA-LHb}$::ChR2 and *TH*$^{VTA-LHb}$::Control mice bilaterally implanted with optical fibers aimed at the LHb were given daily, 1 hr access to operant chambers (Med Associates) interfaced with optogenetic stimulation equipment. Mice were trained on a fixed-ratio 1 training schedule to nose-poke for optical stimulation of *TH*$^{VTA-LHb}$::ChR2 fibers. Each nose-poke in

the active port resulted in a 3-s 20-Hz optical pulse train that was paired with a 3-s tone and houselight cue.

5-choice optical self-stimulation. At least 24 hr following optical self-stimulation, *TH*$^{VTA\text{-}LHb}$::ChR2 and *TH*$^{VTA\text{-}LHb}$::Control mice bilaterally implanted with optical fibers aimed at the LHb were given one, 1-hr session in an operant chamber containing 5 nose-poke ports. A nose-poke in each port would result in a 1-, 5-, 10-, 20-, or 40-Hz optical stimulation. The pairing of the port with the frequency was counterbalanced between mice.

REFERENCES

Donello, J.E., Loeb, J.E., and Hope, T.J. (1998). Woodchuck hepatitis virus contains a tripartite posttranscriptional regulatory element. J. Virol. *72*, 5085–5092.

Livak, K.J., and Schmittgen, T.D. (2001). Analysis of Relative Gene Expression Data Using Real-Time Quantitative PCR and the 2−ΔΔCT Method. Methods *25*, 402–408.

Phend, K.D., Weinberg, R.J., and Rustioni, A. (1992). Techniques to optimize post-embedding single and double staining for amino acid neurotransmitters. J. Histochem. Cytochem. *40*, 1011–1020.

Tritsch, N.X., Ding, J.B., and Sabatini, B.L. (2012). Dopaminergic neurons inhibit striatal output through non-canonical release of GABA. Nature *490*, 262–266.